Organization and Development of Brain Stem Auditory Nuclei of the Chicken: Organization of Projections from N. magnocellularis to N. laminaris

THOMAS N. PARKS AND EDWIN W RUBEL
Department of Psychology, Yale University, New Haven, Connecticut 06520

ABSTRACT The tonotopic and topographic organization of the bilateral projection from second-order auditory neurons of nucleus magnocellularis (NM) to nucleus laminaris (NL) was examined in young chickens. In one group of birds, the NM axons which innervate the contralateral NL were severed by cutting the crossed dorsal cochlear tract at the midline. Heavy terminal degeneration in NL was confined to the neuropil area immediately ventral to the perikaryl lamina. Very little degeneration was seen in the dorsal neuropil region. In a second series of animals, the characteristic frequency (CF) of cells in an area of NM was first determined by microelectrode recording techniques and then a small electrolytic lesion was made through the recording electrode. Following survival periods of 24–48 hours, the distribution of projections from the lesioned area to the ipsilateral and contralateral NL was examined using the Fink-Heimer method.

As previously described in the pigeon, projections from NM terminate densely in the neuropil region immediately dorsal to the ipsilateral NL cell bodies and ventral to the perikaryl layer on the contralateral side, providing each NL neuron with segregated binaural innervation. Lesions in any area of NM produced degeneration confined to a limited caudo-rostral and medio-lateral portion of both laminar nuclei. To investigate this topographic relationship, the caudo-rostral extents of the lesion in NM and of the resulting degeneration in both NL were determined. Linear regression and correlation analyses then related these positional values to each other and to the CF found at the center of each lesion. All correlations were highly significant and ranged from 0.78 between the position of the lesion in NM and CF to 0.91 between the caudo-rostral position of degeneration in the NL ipsilateral and contralateral to the lesion.

It is concluded that neurons in NM project in a very discrete topographic, tonotopic and symmetrical fashion to NL on both sides of the brain, contributing to the binaural response properties and tonotopic organization of neurons in NL. The results also suggest that the organization of projections from NM to NL could provide a mechanism for the differential transmission delay required by a "place" model of low-frequency sound localization.

In birds, the cochlear division of the eighth cranial nerve terminates in a topographic fashion upon two brain stem centers, nucleus angularis (NA) and nucleus magnocellularis (NM). Successively apical portions of the cochlea project to increasingly rostroventral areas in NA and increasingly caudolateral parts of NM (Boord and Rasmussen, '63). Nucleus magnocellularis and the medial division of NA have been considered homologous to the mammalian anteroventral cochlear nucleus (AVCN) and posteroventral cochlear nucleus, respectively (Boord, '68, '69; Rubel and Parks, '75). Axons originating in NM course ventrally and rostrally in the dorsal cochlear tract (CTr) to innervate the dorsal surface of the ipsilateral nucleus laminaris (NL). Other fibers from NM (the crossed dorsal cochlear tract, CTrX) decussate, turn rostrally and end upon the ventral surface of the contralateral NL (Ramón y Cajal, '08). In the adult pigeon, Boord ('68) has confirmed that degenerating axons and axon terminals resulting from interruption of the CTrX are primarily localized to the ventral half of NL.

In the preceding report (Rubel and

Parks, '75) the tonotopic arrangements of NM and NL were described and shown to be strikingly similar. Low frequency stimuli activate cells in caudolateral positions and higher frequencies excite successively rostromedial portions of both nuclei. Linear regression analyses relating the characteristic frequency (CF) of auditory units to their positions within either nucleus indicated that similar functions can be used to account for 79% and 89% of the frequency variance found within NM or NL, respectively. These data suggest that both ipsilateral and contralateral projections from NM maintain a similar and highly-ordered topographic arrangement, giving rise to both the binaural response properties and the tonotopic organization of NL neurons.

The present study sought to directly investigate the relationships between NM and NL in the young chicken, using experimental anatomical techniques. More specifically, this report describes: (1) The position of terminal degeneration in NL resulting from interruption of the contralateral projection from NM, and (2) The tonotopic and topographic organization, and bilateral symmetry of the NM-to-NL projection through the analysis of bilateral degeneration patterns in NL following small electrolytic lesions in physiologically-characterized portions of NM.

MATERIALS AND METHODS

Subjects and histology

Three- to fifteen-day-old chickens of the White Leghorn and Red Cornish breeds were used in all experiments. The animals were anesthetized with a 1.5 ml/kg intraperitoneal injection of Equi-Thesin (Jensen-Salsbery Laboratories). After surgery (see below), animals were maintained in a temperature controlled box at 35°C for 24–48 hours and then sacrificed with a 0.5 ml injection of Equi-Thesin. The animals were perfused transcardially with chicken Ringer's solution for one minute and with 10% formalin for ten minutes. Brains were removed from the skulls and placed in a solution containing 30% sucrose and 10% formalin for five–ten days. The brains were then blocked, sectioned at 25 μ on a freezing microtome and stained by the first method of Fink and Heimer ('67) for degenerating axon terminals or (every third section) with thionin. Sections were maintained in serial order and numbered accordingly.

Crossed dorsal cochlear tract transection

Under aseptic conditions, skin and muscle overlying the supraoccipital area were incised and retracted. A 27 gauge needle was inserted through the foramen magnum and maneuvered in such a way that the axons from NM which form the crossed dorsal cochlear tract were severed. Five animals received this treatment and two others served as controls, having had the needle inserted into the foramen magnum but not so as to cut the CTrX. Following surgery, the incision was closed with alpha-cyanoacrylate adhesive (Aron Alpha, Vigor Corp.).

Nucleus magnocellularis lesions

Surgery. Following induction of anesthesia, the subjects' beaks were fastened to a headholding apparatus with dental acrylic cement. Body temperature was maintained at 39°C and the skin and muscle over the occipital bone were incised and retracted. After ligation of the mid-sagittal sinus, the cerebellum was aspirated to facilitate access to the auditory nuclei. To determine the effects of the cerebellectomy on terminal degeneration in NL, two additional groups were included. In one group (N = 4), animals received a complete cerebellectomy and no other treatment. In the other group (N = 5), animals received lesions in NM from microelectrodes lowered through the intact cerebellum. In all other respects, this second group was identical to the main experimental group (N = 10) described below.

Stimulus presentation and electrophysiological recording. The stimulus presentation and electrophysiological recording techniques have been described in detail (Rubel and Parks, '75). In brief, electrophysiological responses in the left NM were recorded through glass-insulated tungsten microelectrodes with 10–40 micra of exposed tip. While 70 dB (re 0.0002 dynes/cm^2) white noise bursts of 50 msec duration and 10 msec rise and fall times were being presented to the left ear at a rate of 0.67/sec, the microelectrode was lowered into the brain until large acoustically-respon-

sive units characteristic of NM were obtained. The two or three largest-amplitude units in a cluster were selected for determination of characteristic frequency (CF). The CF was first determined "manually" by observing unit activity on the oscilloscope as the stimulus frequency was slowly changed. Unit firing rates to tonal stimuli at this frequency, and approximately 200 Hz above and below, were then assessed from post-stimulus-time histograms constructed over 128 presentations of each stimulus at an intensity 5–20 dB above the response threshold at the manually-determined CF. In most instances, the two procedures resulted in comparable CF values; in the two cases where agreement was not good, the process was repeated until an accurate CF was obtained.

Lesions. Following CF determination, a small electrolytic lesion was made through the recording microelectrode by passing 10–40 micro-amperes of current for 10–25 seconds with the electrode serving as the anode. After the lesion was made and confirmed by the subsequent lack of acoustically-driven unit activity, the skin incision was sutured, the bird was allowed to recover from anesthesia and was maintained at 35°C for 24–48 hours. The animal was then sacrificed and the brain was processed as described above.

Analysis of degeneration. The outline of each stained section was traced using an overhead projector at × 46 and details of terminal degeneration were added to the drawings by viewing the tissue under a × 40 planapochromatic objective (N.A. = 1.0) in a Zeiss WL microscope (total magnification was × 500).

The position of degeneration resulting from each NM lesion was quantitatively analyzed using the following procedure. By observation of the serially-numbered sections, the caudo-rostral and medio-lateral extents of NM and NL were determined, as were regions occupied by the lesion and resulting degeneration grains. Using the method described by Konigsmark ('70) for determining section thickness, it was concluded that there was no significant variation in section thickness within each brain among the Fink-Heimer and the Nissl-stained groups of sections. The position and extent of the lesion (in NM) and degeneration (in each NL) were then expressed as percentile values, from posterior to anterior, within the respective nucleus.

That is, in each animal a lesion was placed in the left NM at a physiologically-characterized position. The caudo-rostral position and extent of the lesion was then expressed as a percentile region within NM along the posterior-anterior dimension of the nucleus. The position and extent of degenerating terminal debris in the ipsilateral and the contralateral NL was similarly expressed as a posterior-to-anterior percentile region with respect to each of these nuclear regions. In this way the relationships between CF, position of the lesion in NM, and positions of degeneration found in each NL could be compared across subjects (fig. 4). This entire procedure was accomplished for 15 subjects receiving discrete NM lesions.

Since the lesions were spherical in most cases, it was assumed that cells at the center of the sphere formed by the lesion were the neurons whose CF was determined just prior to the lesion (cf. Rowland, '66). For the quantitative analyses (relating CF, site of lesion in NM, and the position of degeneration in each NL) the centile points exactly midway between the anterior and posterior boundaries of the lesion and both areas of degeneration were determined for each subject. These positions, referred to as the lesion center-point and degeneration center-points, respectively, were then subjected to linear regression and correlational analyses.

RESULTS

Crossed dorsal cochlear tract transections

In all five animals which received a complete transection of the CTrX, numerous degenerating axons could be seen in the CTrX distal to the transection on both sides of the brain and heavy terminal degeneration was seen covering the ventral neuropil and perikarya of both NL. Very rarely, degenerating fibers could be seen passing through the line of perikarya to end on the dorsal side of NL. Degeneration was observed to extend slightly around the medial edge of NL to occupy a small region both dorsal and ventral to the NL cells. In contrast, the two sham-operated control animals showed no degeneration

on NL. In figure 1, low (A) and high (B) power photomicrographs illustrate the dense degeneration found in the experimental subjects.

Nucleus magnocellularis lesions

Degeneration from a complete cerebellectomy was seen in the restiform body, lateral vestibular nucleus and bulbopontine reticular formation. No degeneration was seen in the auditory nuclei although degenerating fibers pass immediately ventrolateral to the ventral neuropil region of NL at rostral levels.

Other than the absence of degeneration characteristic of the cerebellectomy, no differences were observed between the five animals in which the microelectrode was lowered through the cerebellum and those which received a cerebellectomy prior to the lesion in NM. Thus these groups will be described together.

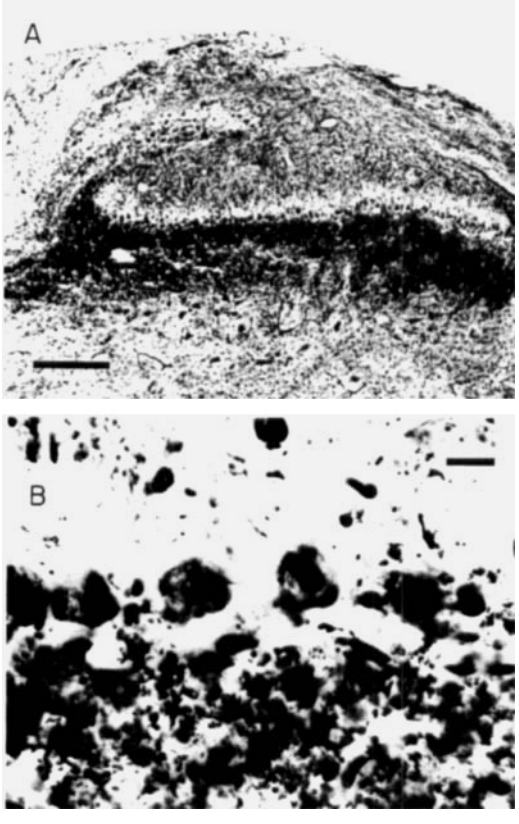

Fig. 1 Photomicrographs showing terminal degeneration in the ventral half of nucleus laminaris (NL) resulting from a midline transection of the crossed dorsal cochlear tract projection from the contralateral nucleus magnocellularis. 25 μ coronal sections, Fink-Heimer stain; medial is to the left. A, low-power view, bar indicates 0.2 mm. B, high-power view of same section, bar indicates 20 μ.

The CFs of the units at the center of the lesions in NM ranged from 0.57 kHz to 3.03 kHz, or over 60% of the audible range reported for many birds (Schwartzkopff, '68; Rubel and Parks, '75). The lesions encompassed from 18–55% of the rostrocaudal extent of NM and occupied varying portions of both the medial and lateral divisions of NM in caudal placements and the medial division alone in more rostral sites.

Figures 2 and 3 show, in detail, the results obtained from a representative animal, 74-895. In this subject the NM lesion was at a position where the CF was 1.0 kHz. In figure 2, serial tracings of coronal sections through the brainstem indicate the placement of the lesion in NM (blackened area) and the positions at which terminal degeneration was seen (stippled areas) in both laminar nuclei. Note that the lesion, in succeedingly rostral sections, occupies progressively lateral portions of NM. Similarly, the resulting degeneration in both NL occupies successively lateral areas at increasingly rostral positions. The photomicrographs in figure 3 show a Nissl-stained section through the lesion (A) and silver-stained sections of the terminal degeneration; in the dorsal neuropil area of NL ipsilateral to the lesion (B) and in the ventral neuropil area of NL contralateral to the lesion (C).

Each panel in figure 4 summarizes the data obtained from one animal. The animal identification number and the CF determined at the lesion site in NM are noted on the left portion of each panel. The respective percentile extents of the lesion in NM and degeneration in both NL are shown on the right. The panel for animal 74-895, for example, shows a CF of 1.0 kHz and a lesion which extended from the sixteenth to the fifty-third posterior-to-anterior centile of the nucleus. The resulting degeneration on the NL contralateral to the lesion extended from the twentieth to the forty-fifth centile. The panels are arranged in order of increasing CF. Electrode punctures in the rostral

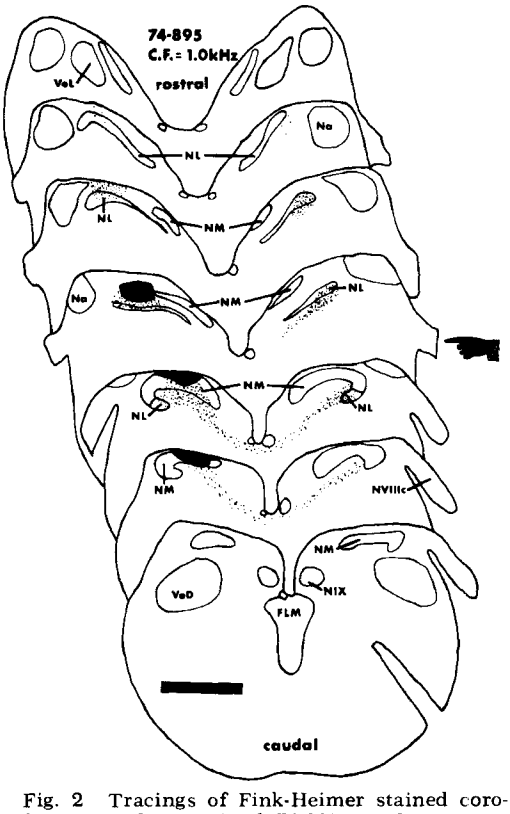

Fig. 2 Tracings of Fink-Heimer stained coronal sections from animal 74-895, used to reconstruct positions of lesion in nucleus magnocellularis (NM) and resulting degeneration in both nuclei laminaris (NL). The sections shown here extend, at irregular intervals, from the most caudal section containing NM to the rostral pole of NL. The characteristic frequency (CF) of units at the center of the lesion in NM was 1.0 kHz. Lesioned area is indicated in black, degeneration as dots. Note that, at rostral levels, both lesion and degeneration occupy lateral portions of NM and NL, respectively. Pointer indicates section from which figures 3B,C were taken and bar indicates 1.0 mm. FLM, fasciculus longitudinalis medialis; Na, nucleus angularis; NIX, nucleus nervi glossopharyngei; NVIIIc, nervus octavus, pars cochlearis; VeD, nucleus vestibularis descendens; VeL, nucleus vestibularis lateralis.

half of NM obtained units with CF's above approximately 1.5 kHz while posterior punctures obtained units with CF's below 1.5 kHz. Lesions in the rostral half of NM produced degeneration in the rostral halves of the two NL while posterior lesions produced degeneration caudally in NL. Although the medio-lateral dimension of NM and NL was not treated quantitatively, several animals had lesions in NM which did not involve the entire medio-lateral extent of the nucleus. As shown in figure 2 for animal 74-895, these partial lesions produced degeneration in portions of both NL analogous to the portion of NM destroyed. That is, lateral lesions produced lateral degeneration and more medial lesions yielded more medial degeneration on *both* the ipsilateral and contralateral NL.

When the total extents of the lesions and resulting degeneration are compared there is considerable variability. In some brains (e.g. 74-885), the degeneration appears to cover more than twice as great a percentage of NL as the lesion destroyed in NM. In other cases (e.g. 74-850), the extent of degeneration on ipsilateral and contralateral NL are quite different, although in most instances they are similar.

The lesion and degeneration center-points were plotted against each other and against CF's to yield measures of tonotopic organization in NM and of tonotopic and topographic organization of NM's innervation of both laminar nuclei. These plots comprise figures 5–8. The line of best fit (least squared deviations) was determined for each plot and (in figs. 5–7) the regressions were tested for a linear relationship. The line equation and standard error of estimate are shown in each case. In figure 8, a correlation coefficient was calculated and its significance tested. In all cases, the results were highly statistically significant ($df = 13$ and p's < 0.001).

Figure 5 indicates that 61.4% of the variance in CF was accounted for by the caudo-rostral position of the lesion in NM, suggesting that the tonotopic organization of NM reported earlier (Rubel and Parks, '75) was apparent in these animals as well.

Figure 6 shows the relationships between CF at the position of the lesion and the center-points of degeneration found in NL ipsilateral (NLi) and contralateral (NLc) to the lesion. CF accounts for 74.3% and 62.8% of the variance in degeneration position found in NLi and NLc, respectively. Therefore, the characteristic frequency of a cell group in NM is a reliable indicator of the areas in both NL to which those cells project; that is, the tonotopic organization of NM is maintained in its projections to the ipsilateral and contralateral NL.

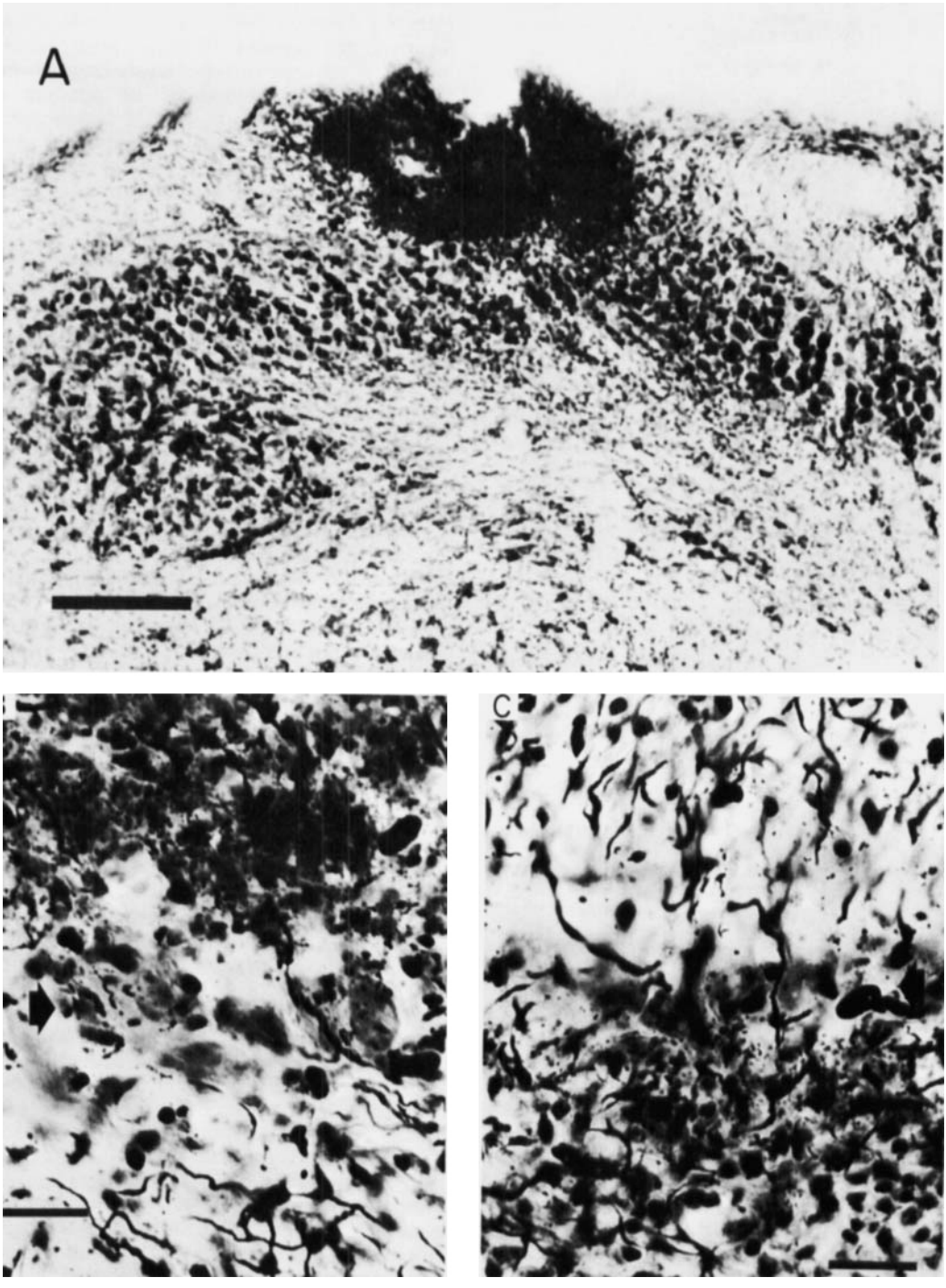

Fig. 3 Photomicrographs from animal 74-895 showing the lesion in the left nucleus magnocellularis and resulting degeneration in both nuclei laminaris (NL). 25 μ coronal sections. B and C were taken from the section indicated by the pointer in figure 2. A, lesion occupying dorsal portion of the caudal NM. Medial is to the right; thionin stain, bar indicates 0.2 mm. B and C, terminal degeneration and an increased number of glial cells lying dorsal to cell bodies of the NL ipsilateral to the lesion (B) and ventral to cell bodies of the contralateral NL (C). Fink-Heimer stain; bars indicate 40 μ and arrows indicate the position of NL perikarya.

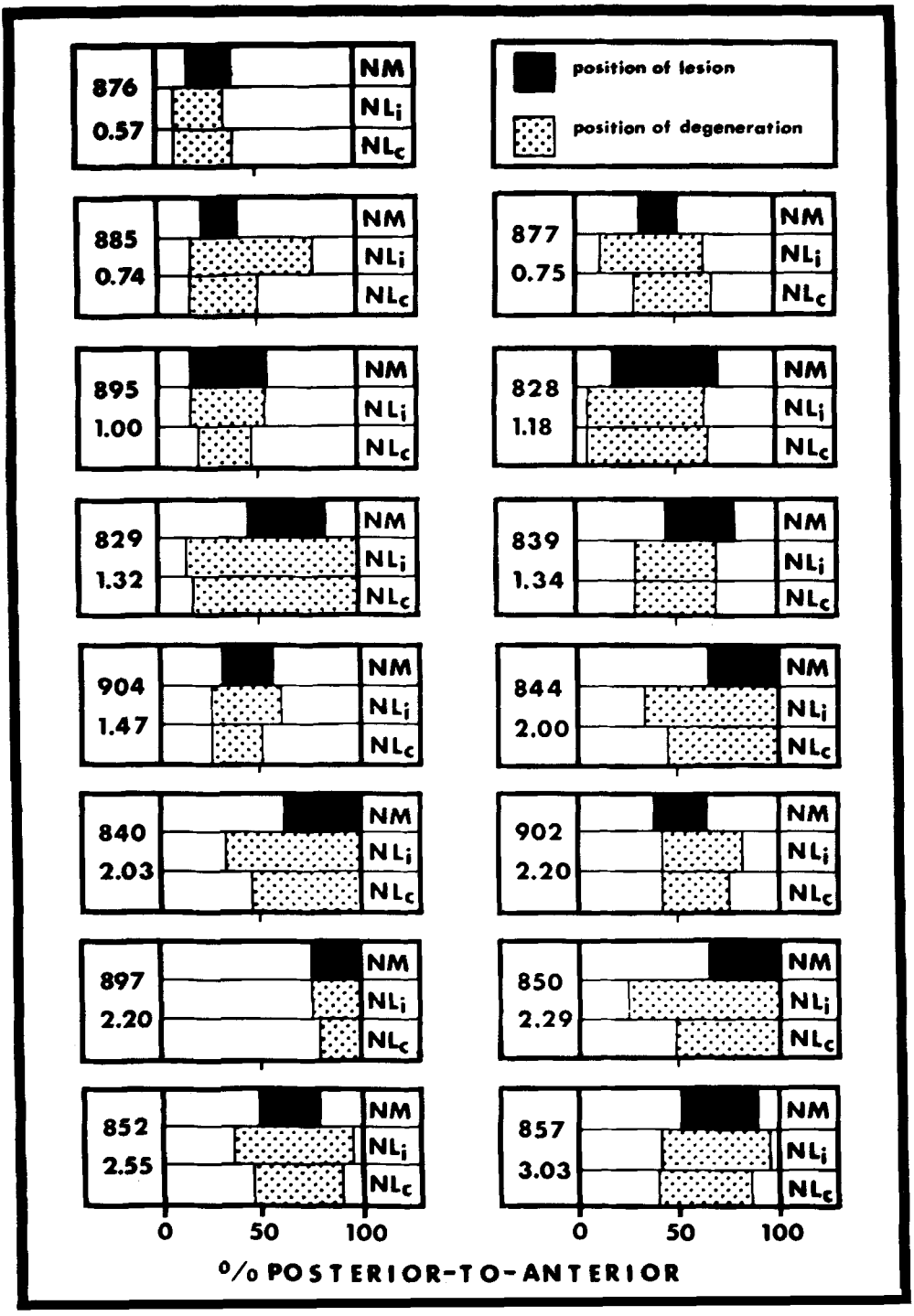

Fig. 4 Panels showing the percentage positions of the electrolytic lesion in nucleus magnocellularis (NM) and terminal degeneration in both nuclei laminaris (NL) for each of fifteen animals. The top bar in each panel represents the total caudo-rostral extent of NM from 0–100%. The area destroyed by the lesion is denoted in black. The second and third bars in each panel represent the caudo-rostral extent (0–100%) of nucleus laminaris ipsilateral (NLi) and contralateral (NLc) to the lesion, respectively. The position of silver-stained degeneration within each NL is denoted by stippling. To the left of the bars in each panel are the animal identification number and the characteristic frequency (in kHz) of the units at the center of the lesion in NM. The prefix "74," which denotes the year in which the experiments were performed, has been omitted from the animal identification numbers in this figure.

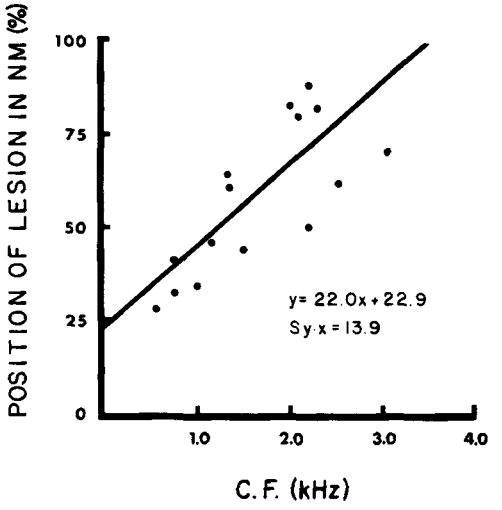

Fig. 5 Scatter-plot and linear regression relating lesion position in NM to characteristic frequency (CF) of units at center of lesion. The regression equation and standard error of estimate are shown.

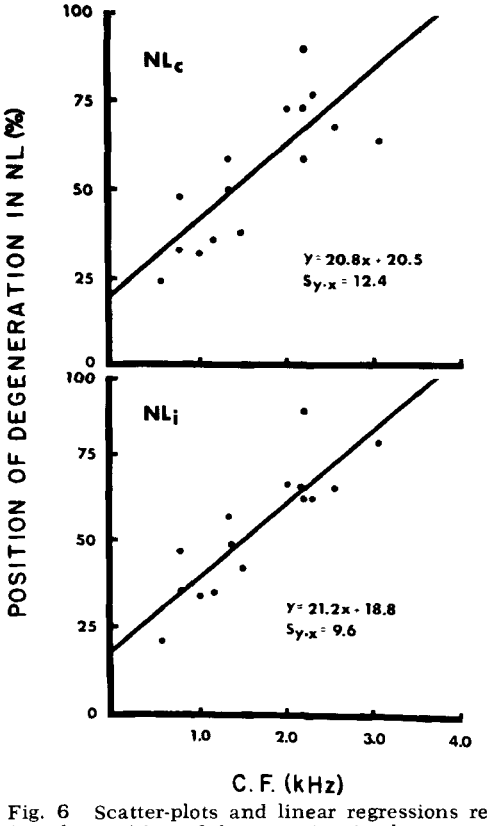

Fig. 6 Scatter-plots and linear regressions relating the position of degeneration in the contralateral and ipsilateral nucleus laminaris (NLc and NLi, top and bottom graphs, respectively) to the characteristic frequency (CF) of units at the center of the lesion in n. magnocellularis. The regression equations and standard errors of estimate are shown.

Similarly, as shown in figure 7, the position of the NM lesion is strongly related to the caudo-rostral position of degenerating terminals in NLi and NLc, accounting for 72.8% and 89.6% of the variance, respectively. Thus, projections from NM to each NL maintain a highly ordered topographic, as well as tonotopic, arrangement.

Finally, figure 8 shows a scatter-plot relating the caudo-rostral center-points of degeneration in the ipsilateral and contralateral NL and the least-square line of best fit. A product-moment correlation of 0.91 indicates that projections from regions in NM innervate corresponding caudo-rostral positions in the two laminar nuclei.

DISCUSSION

Nucleus magnocellularis is usually described as containing three subdivisions: a medial division with spherical cells of 20–25 μm diameter, a lateral division of similar neurons 18–24 μm in diameter and a ventrolateral region of small stellate and fusiform cells (Boord and Rasmussen, '63). The medial division of NM receives innervation from the basal two-thirds of the cochlea while the apical one-third of the cochlea projects to the lateral division of NM (Boord and Rasmussen, '63). Boord ('68) concluded that in the pigeon only the medial portion of NM sends axons into the dorsal cochlear tracts but noted that, "while it would appear reasonable that the lateral part also projects bilaterally to NL, this could not be demonstrated" (p. 528). The present study confirms and extends the findings of Boord ('68) that the NM axons forming the two dorsal cochlear tracts produce binaural, spatially-segregated innervation of NL. It is now apparent that fibers forming the uncrossed dorsal cochlear tract descend *in register* to the dorsal surface of the ipsilateral NL, maintaining, to a great degree, the cochleotopic innervation of NM. The crossed dorsal cochlear tract fibers

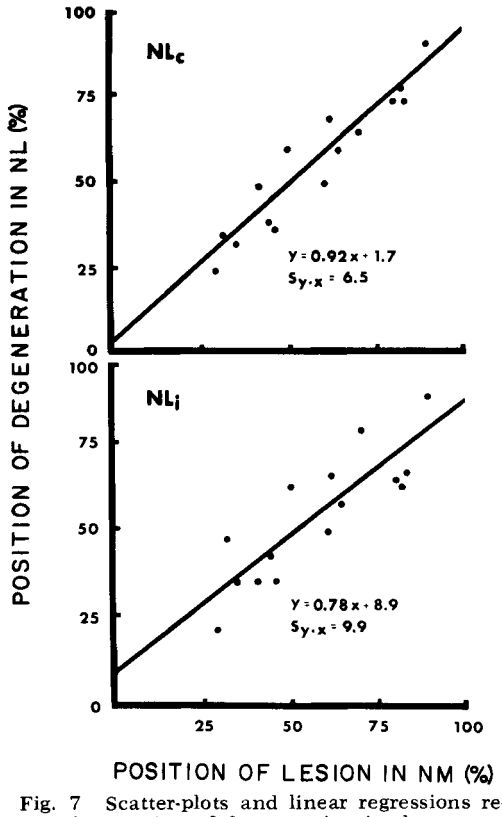

Fig. 7 Scatter-plots and linear regressions relating the position of degeneration in the contralateral and ipsilateral nucleus laminaris (NLc and NLi, top and bottom graphs, respectively) to the position of the lesion in nucleus magnocellularis. The regression equations and standard errors of estimate are shown.

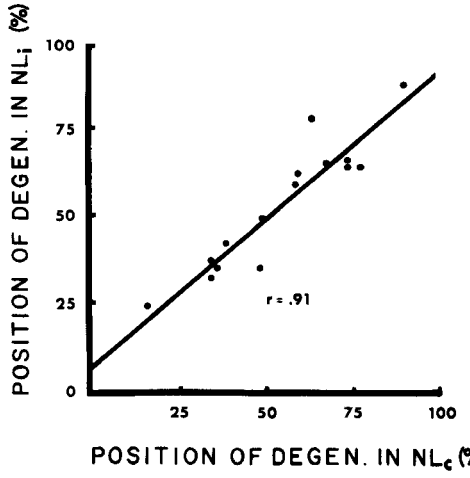

Fig. 8 Scatter-plot and line of best fit relating the respective positions of degeneration in nucleus laminaris ipsilateral (NLi) and contralateral (NLc) for each lesion in nucleus magnocellularis. The correlation coefficient is shown.

cross the midline and turn rostrally to effect a corresponding topographic innervation on the ventral surface of the contralateral NL. Furthermore, the results of this study and the demonstration by Rubel and Parks ('75) of units in NL with CF's below 0.5 kHz suggest that (in addition to its contributions to the trapezoid body) NM pars lateralis does send fibers through both dorsal cochlear tracts to innervate NL on each side of the brain stem.

The relationships between the loci of degeneration in the laminar nuclei, the CF at the lesion position, and the locus of the lesion in NM indicate that there is considerable functional and topographic specificity in the organization of connections from NM to NL. When the tonotopic organization of the ipsilateral and contralateral projection to NL are considered by regressing CF on the positions of degeneration in each NL (i.e. exchange ordinates and abscissae in figure 6) the slopes of the regression lines are 0.035 and 0.030 for NLi and NLc, respectively. These values compare favorably with the slope found using microelectrode mapping methods (Rubel and Parks, '75). Furthermore, the consistent relationship between lesion position and location of degeneration in NL along with the high correlation between the positions of ipsilateral and contralateral degeneration imply that the tonotopic organization of NL results from the topography of NM projections. These data clearly indicate that each area of NL receives spatially-separated innervation from essentially identical points in the two magnocellular nuclei and, by extension, from corresponding loci in both cochleae.

Whether this bilateral projection from NM is due to bifurcation of each axon to join both the CTr and the CTrX (as suggested by Ramón y Cajal, '71) or from different cells lying in the same area of NM, is not clear. In either case, the mechanisms by which axons from a specific site in NM come to occupy corresponding positions on both NL are of interest. In this regard Gaze ('70) suggests that functional interaction between neural elements "simultaneously receiving similar spatiotem-

poral patterns of excitation" allows points on the two optic tecta of anurans to become connected during development. Similar processes might account for the specificity of the dorsal cochlear tract projections. As Gaze ('70) noted, the functional interaction hypothesis is attractive because it is subject to experimental invalidation, in the present case through appropriate manipulations of the auditory experience of the two ears.

Uncontrolled sources of variation

From 61–90% of the variance in the dependent variables of this study (i.e. CF or position of degeneration in NL) was accounted for by the independent variables (i.e. CF or position of the lesion in NM). There are several reasons to believe that the relationships between CF, lesion position in NM and position of degeneration on NL are, in fact, even more precise. Probably the most important source of uncontrolled variation is that, due to fibers of passage, a lesion placed medially in NM will interrupt more fibers in the crossed dorsal cochlear tract than a laterally-placed lesion, whereas a lateral lesion may interrupt more ipsilateral than contralateral projections. Thus, in the present study, only the caudo-rostral dimension of NM and NL could be quantitatively considered. Since Rubel and Parks ('75) have shown that the tonotopic organization of each nucleus extends from caudolateral to rostromedial and a medio-lateral specificity in NM projections to each NL was observed in this study, it is certain that the medio-lateral position of the lesion is an important source of uncontrolled variation. Second, in relatively thick frozen sections it is not possible to precisely determine the boundaries of either a lesion or degeneration. Thus small differences in measurement criteria will introduce further variation. Third, CF determination was probably accurate to within only about 100 Hz. Finally, since each data point is contributed by a different animal, differences due to age, weight and sectioning angle are to be expected.

Comparisons with other amniotes

Although nuclei similar in cytoarchitecture and afferent connections to the avian NM are found in a variety of reptiles (Leake, '74; DeFina and Webster, '74; Miller, '75) the existence of a well-defined reptilian NL has been established only in the case of *Caiman* (Leake, '74) and the Tegu lizard, *Tupinambis nigropunctatis* (DeFina and Webster, '74). Miller tentatively identified a rudimentary NL in some lizards but concluded that the nucleus does not appear unequivocally in any of the fourteen species he examined. In those reptiles where a well-defined NL exists, it is similar in position and structure to its avian counterpart, though there is little knowledge of the laminar nucleus' afferent or efferent connections in any reptile (Miller, '75).

On the basis of cellular organization, dendritic configuration and connections, Ramón y Cajal concluded that, "the acoustic centers of birds are built on the same plan as those of mammals. They have changed only in shape and position in order to adapt to the configuration and the extent of other nuclei and bulbar tracts . . ." (Ramón y Cajal, '71, p. 119). Thus, n. magnocellularis and n. angularis have been considered homologous to the cochlear nuclei of mammals (Boord, '69) and NL has been associated with the mammalian medial superior olivary nucleus (MSO). The suggested homology between NL and the MSO has also received support from experimental anatomical studies demonstrating that NL neurons receive polarized afferents from both magnocellular nuclei (Boord, '68) and are not innervated directly by the cochlear ganglion (Boord and Rasmussen, '63). In addition, cells in both NL and the MSO show similar electrophysiological response properties (Goldberg and Brown, '68, '69; Schwartzkopff, '68; Guinan et al., '72a; Rubel and Parks, '75).

Warr ('66), Goldberg and Brown ('68), van Noort ('69) and Strominger and Strominger ('71) have studied anterograde degeneration following anteroventral cochlear nucleus lesions in dogs, cats and monkeys. These studies share the limitation that lesions produced in the AVCN were often quite large and inclusive of surrounding structures. Taken together, however, the data establish the existence of a topographic projection from the AVCN to the MSO. The present demonstration of a very discrete topographic organization in the

projections of NM to NL, therefore, adds further support to the notion of a homologous relationship between the avian NL and the mammalian MSO.

The morphological and physiological similarities between NL and the MSO provoke consideration of their function in audition. Considerable evidence indicates that the MSO is a major participant in the spatial localization of low-frequency sound (Erulkar, '72; Masterton et al., '75). Less substantial data support a similar role for the avian NL (Erulkar, '72). For example, the number of neurons and the complexity of their arrangement in NL is greatly increased in several species of birds whose outstanding behavioral specialization is heightened accuracy in sound localization. In *Tyto alba*, a night-hunting owl with asymmetric ears, the number of cells in NL is about ten thousand, while a falcon of similar size, *Falco tinnunculus*, has only two thousand cells in each NL (Schwartzkopff, '68). Hollander ('71) demonstrated a significant but less dramatic hypertrophy of NL in the echolocating species of the cave swiftlet genus *Collocalia*.

Nucleus laminaris and low-frequency sound localization

It is now generally accepted (Erulkar, '72; Gulick, '71) that there are two principal cues for determining the azimuth of a sound source: the difference in time of arrival of the sound at the two ears ("Δt") and the difference in the frequency-intensity spectra of the sounds at the two ears ("Δfi"). Furthermore, a variety of studies on human and animal sound localization indicate that for lower sound frequencies Δt is the primary localization cue, while Δfi is the relevant parameter for high frequencies. Recent investigations of the mammalian superior olivary complex, using neurophysiological, lesion, and comparative anatomical and behavioral methods, strongly suggest that the lateral superior olivary nucleus is chiefly responsible for analysis of Δfi cues for high-frequency sounds and that the medial superior olivary nucleus (MSO) is primarily an analyzer of Δt information for lower frequency stimuli (Goldberg and Brown, '68, '69; Guinan et al., '72a,b; Masterton, '74). In view of the many structural and physiological similarities between the MSO and NL (as discussed in a previous section) and the fact that many birds do not hear above 5 kHz, it seems likely that NL is involved in the analysis of Δt information for low-frequency stimuli (Erulkar, '72).

Some years ago, Jeffress ('48) proposed a theory of sound localization which allowed specific differences in the time of a stimulus' arrival at the two ears (i.e. specific Δt's) to be coded at particular places in the central nervous system. As elaborated by Licklider ('59), Goldberg and Brown ('69) and others, this "place" theory of low-frequency sound localization rests on several basic assumptions:

(1) Second-order auditory fibers are exclusively excitatory and are phase-locked to the stimulus.

(2) The third-order auditory cell fires maximally when *simultaneously* activated by ipsilateral and contralateral second-order neurons.

(3) There are differential transmission delays between the two inputs to each third-order neuron so that for each Δt, there is a particular place in the third-order nucleus where cells receive simultaneous binaural stimulation at just that Δt.

All of these basic assumptions have received at least some experimental support. Neurons in the AVCN are often phase-locked to tonal stimuli (Goldberg and Brownell, '73; Kiang et al., '73). Physiological recording from cells within the mammalian MSO has also demonstrated that there are cells within this nucleus which receive excitatory input from both AVCN, are phase-locked to a stimulating sinusoid and whose firing rate is a continuous function of interaural delay (Goldberg and Brown, '69; Guinan et al., '72a,b). These MSO cells all had CF's below 4.0–5.0 kHz. Although the mechanism of differential delay is unclear, Goldberg and Brown ('69) indicate that the Δt's most and least favorable to firing rate are relatively unaffected by variations in average binaural intensity or by interaural intensity differences. These authors also argue that for binaural MSO cells, the value of the most favorable delay should be relatively unaffected by variations in tonal frequency over a limited frequency range. According to Goldberg and Brown, such

characteristics are consistent with the idea that each such neuron is a "coincidence detector" (i.e. a detector of a particular Δt). Any of a variety of mechanisms (e.g. anatomical arrangements or synaptic interactions within the transmission nuclei) might account for the differential delay necessary to explain the Δt-dependent firing rate. Differential second-order axon diameter (and thus conduction velocity) has been suggested as one possible mechanism (Moushegian et al., '67). On the other hand, it now appears unlikely that synaptic interaction sufficiently complex to account for the delay times involved occurs in the AVCN (Goldberg and Brownell, '73). The present discussion deals with only one of the several possible mechanisms of differential delay.

In the preceding paper (Rubel and Parks, '75) we demonstrated that NM and NL of the chicken have similar functional organizations. Quantitative analyses indicated that the major axis of tonototopic organization in each nucleus is from caudolateral (low frequencies) to rostromedial (high frequencies). NM may thus be seen as a series of "isofrequency planes" or "slabs" of neurons running from caudomedial to rostrolateral and having similar CF's. NL (as a single cell lamina) is composed of a series of "isofrequency bands," also oriented along the caudomedial-to-rostrolateral dimension. The results of the present study suggest that NM projects in a point-to-point fashion onto both NL. Thus, within each isofrequency band, NL neurons receive topographically-organized bilateral projections from NM: caudomedially-situated NL neurons receive afferents from caudomedial areas of each NM and rostrolateral NL cells receive afferents from rostrolateral positions in each NM. The existence of this projection pattern within each NL isofrequency band leads to the question of its biological significance. What information, if any, is coded along each isofrequency band of NL neurons (i.e. orthogonal to the tonotopic axis of NL)?

Due to the topographic projection discussed above, the lengths of axons from NM to the contralateral NL (i.e. axons in the CTrX) decrease gradually from the lateral edge of NL medially. The lengths of the ipsilateral (CTr) fibers, however, probably vary little within each isofrequency band (cf. Rubel and Parks, '75; fig. 1). If we let Δd equal the difference in lengths of contralateral and ipsilateral projections to any NL neuron, then within each isofrequency band Δd is large rostrolaterally and progressively smaller caudomedially. Assuming equal conduction velocities (v) in the ipsilateral and contralateral projections from NM to NL, the transmission delay (t') from NM to the dendrite of an NL neuron will be proportional to the axonal distance. Thus, each NL neuron within an isofrequency band will have a differential transmission delay to its dorsal and ventral dendritic areas ($\Delta t'$) which will equal $\Delta d/v$. That is, for each cell in NL there will be a $\Delta t' = \Delta d/v$ and $\Delta t'$ will vary systematically along each isofrequency band, with high values found rostrolaterally and low values caudomedially. Therefore, for any sound source located to one side of the median plane (i.e. $\Delta t > 0$), there could be one place in the contralateral NL where $\Delta t' = \Delta t$. Only at this place in NL would neurons receive simultaneous stimulation of their dorsal and ventral dendrites. In this way, a series of Δt's might be coded along each isofrequency band in NL by virtue of the differential lengths of the two dorsal cochlear tract projections. And, it follows, the position of each low-frequency sound source in the horizontal plane might be initially coded at a particular place in NL. In that event, sound sources located near the median plane would have a representation more medially in NL (their Δt being smaller) than sources of greater azimuth.

Some preliminary observations on the chicken (Parks and Rubel, unpublished observations) indicate that transmission delays produced by this arrangement could correspond to time differences found at the two ears. The diameter of a twelve-day-old chicken's head is about two centimeters, a distance yielding a maximum interaural time difference (Δt_{max}) of about 100 μsec for a sound source at 90 or 270 degrees of azimuth (Gulick, '71). Measurements made on the medulla of a twelve-day-old chicken brain (fixed for 5 days in a 4% glutaraldehyde-4% paraformaldehyde solution in 0.1 M cacodylate buffer at pH 7.4) indicate that the maximum

length of the crossed dorsal cochlear tract, from the lateral edge of NM to the lateral edge of the contralateral NL, is about 4.0 mm. The maximum length of the ipsilateral dorsal cochlear tract was similarly determined to be about 0.4 mm, giving a maximum Δd of about 3.6 mm. The average diameter of the myelinated axons in both dorsal cochlear tracts appears to be about 2.5 μm (Benes, Parks and Rubel, unpublished observations) which would yield a conduction velocity of about 15 m/sec (Ruch et al., '65). With a maximum differential length of 3.6 mm and an average conduction velocity of 15 m/sec the maximum $\Delta t'$ obtainable would be $\Delta d/v =$ 240 μsec, an adequate time delay to accommodate the 100 μsec Δtmax in a bird of this size.

It is incontestable that some aspects of sound localization behavior in many species depend upon complex stimulus parameters not considered in the model presented above (Erulkar, '72). It is also true that the hypothesis depends upon a number of simplifying assumptions, none of which has been demonstrated. For example, there is no published evidence that NM cells "phase-lock," or that NL cells show "characteristic delays" (see Rose et al., '66) similar to MSO neurons. Furthermore, variability in delays produced by the cochlea or in NM could mask the time differences contributed by differences in the length of the crossed and uncrossed dorsal cochlear tracts. Finally, although the model presented here may have some relevance for sound localization in birds, mammals may use different mechanisms. Nevertheless, the available evidence suggests that the MSO and its avian homologue, NL, are involved in the analysis of Δt for spatial localization of low-frequency sound and that the electrophysiological response properties of neurons in these third-order nuclei are similar to those required of the third-order element in a place theory of sound localization. The hypothesis proposed here suggests a possible mechanism whereby the position of a sound source could be systematically coded on an array of NL neurons. More importantly, this model allows three specific predictions, all subject to direct experimental validation:

1. The activity of NL neurons will vary as a function of the interaural time difference (Δt) of a binaurally-presented stimulus, i.e. cells in NL will show a "characteristic delay."

2. The time difference producing maximal response of NL neurons will increase gradually as progressively rostrolateral sites within an isofrequency band are explored, i.e., optimal Δt will vary systematically in the nuclear dimension orthogonal to the tonotopic gradient described by Rubel and Parks ('75).

3. The "Δt map" will be primarily contralateral since a sound source located to one side of the median plane will affect the dorsal and ventral dendrites of only the contralateral NL simultaneously.

ACKNOWLEDGMENTS

The authors are grateful to Dr. Charles R. Watson for valuable suggestions, to Mr. James E. Cox for advice on statistical matters, to Messrs. Fred Davis, Nigel Cox and Gus Ogren for construction and maintenance of apparatus, to M. Ostapoff, T. Powley and L. Uphouse for criticisms of the manuscript and to Ms. Joan MacDonald for secretarial help. Raoul Garcia y Vega's skilled assistance is also acknowledged. Supported by Grant No. GB 31934 from the National Science Foundation.

LITERATURE CITED

Boord, R. L. 1968 Ascending projections of the primary cochlear nuclei and nucleus laminaris in the pigeon. J. Comp. Neur., *133*: 523–542.

——— 1969 The anatomy of the avian auditory system. Ann. N. Y. Acad. Sci., *167*: 186–198.

Boord, R. L., and G. L. Rasmussen 1963 Projection of the cochlear and lagenar nerves on the cochlear nuclei of the pigeon. J. Comp. Neur., *120*: 463–475.

DeFina, A. V., and D. B. Webster 1974 Projections of the intraotic ganglion to the medullary nuclei in the Tegu lizard, *Tupinambis nigropunctatis*. Brain Behav. Evol., *10*: 197–211.

Erulkar, S. D. 1972 Comparative aspects of spatial localization of sound. Physiol. Rev., *52 (1)*: 237–360.

Fink, R. P., and L. Heimer 1967 Two methods for selective silver impregnation of degenerating axons and their synaptic endings in the central nervous system. Brain Res., *4*: 369–374.

Gaze, R. M. 1970 The Formation of Nerve Connections. Academic Press, London, pp. 253–258.

Goldberg, J. M., and P. B. Brown 1968 Functional organization of the dog superior olivary complex: an anatomical and electrophysiological study. J. Neurophysiol., *31*: 649–656.

Goldberg, J. M., and P. B. Brown 1969 Re-

sponse of binaural neurons of dog superior olive complex to dichotic tone stimuli: Some physiological mechanisms of sound localization. J. Neurophysiol., *32:* 613–636.

Goldberg, J. M., and W. E. Brownell 1973 Discharge characteristics of neurons in anteroventral and dorsal cochlear nuclei of cat. Brain Res., *64:* 35–54.

Guinan, J. J., S. S. Guinan and B. E. Norris 1972a Single auditory units in the superior olivary complex. I. Responses to sounds and classifications based on physiological properties. Int. J. Neurosci., *4:* 101–120.

Guinan, J. J., B. E. Norris and S. S. Guinan 1972b Single auditory units in the superior olivary complex. *II. Locations of unit categories and* tonotopic organization. Int. J. Neurosci., *4:* 147–166.

Gulick, W. L. 1971 Hearing: Physiology and Psychophysics. Oxford Univ. Press, New York.

Hollander, P. 1971 Adaptations for echolocation in cave swiftlets (*Collocalia*). Unpublished doctoral dissertation, Yale University.

Jeffress, L. A. 1948 A place theory of sound localization. J. Comp. Physiol. Psychol., *41:* 35–39.

Kiang, N. Y. S., D. K. Morest, D. A. Godfrey, J. J. Guinan and E. C. Kane 1973 Stimulus coding at caudal levels of the cat's nervous system: I. Response characteristics of single units. In: Basic Mechanisms in Hearing. A. R. Moller, ed. Academic Press, New York.

Konigsmark, R. W. 1970 Methods for the counting of neurons. In: Contemporary Research Methods in Neuroanatomy. W. J. H. Nauta and S. O. E. Ebbesson, eds. Springer-Verlag, New York, pp. 315–340.

Leake, P. A. 1974 Central projections of the statoacoustic nerve in *Caiman crocodilus*. Brain Behav. Evol., *10:* 170–196.

Licklider, J. C. R. 1959 Three auditory theories. In: Psychology: A Study of a Science. Vol. I. S. Koch, ed. McGraw-Hill, New York.

Masterton, R. B. 1974 Adaptation for sound localization in the ear and brainstem of mammals. Fed. Proc., *33 (8):* 1904–1910.

Masterton, B., G. C. Thompson, J. E. Bechtold and M. J. RoBards 1975 Neuroanatomical basis of binaural phase-difference analysis for sound localization: A comparative study. J. Comp. Physiol. Psychol., *89 (5):* 379–386.

Miller, M. R. 1975 The cochlear nuclei of lizards. J. Comp. Neur., *159:* 375–406.

Moushegian, G., A. L. Rupert and T. L. Langford 1967 Stimulus coding by medial superior olivary neurons. J. Neurophysiol., *30:* 1239–1261.

Ramón y Cajal, S. 1908 Les ganglions terminaux du nerf acoustique des oiseaux. Trab. Inst. Cajal Invest. Biol., *6:* 195–225.

——— 1971 [The Acoustic Nerve: Its Cochlear Branch or Cochlear Nerve]. Translated from: Histologie du Systeme Nerveux de l'Homme et des Vertebres. Tome I, pp. 774–838, 1952. (National Technical Information Service Publication No. PB 205 473).

Rose, J. E., N. B. Gross, C. D. Geisler and J. E. Hind 1966 Some neural mechanisms in the inferior colliculus of the cat which may be relevant to localization of a sound source. J. Neurophysiol., *29:* 288–314.

Rowland, V. 1966 Stereotaxic techniques and the production of lesions. In: Neuroendocrinology. Vol. I. L. Martini and W. F. Ganong, eds. Academic Press, New York.

Rubel, E. W, and T. N. Parks 1975 Organization and development of brain stem auditory nuclei of the chicken: Tonotopic organization of N. Magnocellularis and N. Laminaris, J. Comp. Neur., *164:* 411–434.

Ruch, T. C., H. D. Patton, J. W. Woodbury and A. L. Towe 1965 Neurophysiology. W. B. Saunders, Philadelphia, pp. 78–79.

Schwartzkopff, J. 1968 Structure and function of the ear and of the auditory brain areas in birds. In: Hearing Mechanisms in Vertebrates, A Ciba Foundation Symposium. A. V. S. de Reuck and J. Knight, eds. J. & A. Churchill Ltd., London, pp. 41–59.

Strominger, N. L., and A. I. Strominger 1971 Ascending brain stem projections of the anteroventral cochlear nucleus in the rhesus monkey. J. Comp. Neur., *143:* 217–242.

van Noort, J. 1969 The Structure and Connections of the Inferior Colliculus. Van Corcum, Assen.

Warr, W. B. 1966 Fiber degeneration following lesions in the anterior ventral cochlear nucleus of the cat. Exp. Neur., *14:* 453–474.